JOURNAL OF CATALYSIS 122, 1–9 (1990)

Preparation and Characterization of Bimetallic Oxides of Chromium and Titanium

SOOFIN CHENG[1] AND SHENG-YUAN CHENG

Department of Chemistry, National Taiwan University, Taipei, Taiwan, Republic of China

Received October 19, 1988; revised February 22, 1989

Mixed oxides of Cr(III) and Ti(IV) were prepared by the hydrothermal method in basic solutions (pH > 12). With NaOH as base, the resultant materials had a layered structure. After exchange with NH_4^+ ions and calcination at 623 K, the layered structure was converted to the anatase phase. When the calcination temperature was raised to 723 K and higher, a portion of the anatase phase was converted to the rutile phase for samples of high Cr(III) content. The latter also contained a small amount of Cr_2O_3 structure. When the 2-propanol decomposition reaction was carried out, the mixed oxides demonstrated both acidic and basic sites on the surfaces. Furthermore, both Brønsted and Lewis acid sites were found on the surface of the bimetallic oxides, based on IR spectra of the adsorbed pyridine. The Brønsted acid sites were identified as CrO–H groups. When the bimetallic oxides were used as catalysts in oxidative dehydrogenation of ethane, activity was found to be a function of Cr content. The Cr–O species were proposed to be the active sites for formation of both ethylene and CO_2. Titanium served as a diluent. © 1990 Academic Press, Inc.

INTRODUCTION

Oxides of silicon and aluminum are well-known acid catalysts because of their capability in proton transfer and are widely used as catalysts in modern chemical industry. On the other hand, oxides of transition and post-transition metal elements are widely used in redox reactions because of their ability to take part in the exchange of electrons. In addition, highly dispersed metallic catalysts are usually supported over metal oxides to expose their effective surface areas. Typical catalyst supports in common use are Al_2O_3, SiO_2, zeolite, and active carbon. In the 1970s a TiO_2-based catalyst was first applied commercially in air pollution control equipment and became the subject of many scientific studies. Because TiO_2 is easily reduced to form various stoichiometric and nonstoichiometric lower oxides, some distinguishing catalytic properties are expected when it is used as catalyst support. Indeed, the so-called strong metal–support interaction (SMSI) was first reported for noble metals supported on TiO_2 (*1*). The TiO_2-based catalyst was found to be the best catalyst for the selective catalytic reduction of NO_x with NH_3 (*2*), and for partial oxidation of benzene to maleic anhydride (*3*).

Compared to commonly available Al_2O_3 and SiO_2, titania has relatively low acidity and very few acidic sites on the surface (*4*). To improve the acidity, Shibata *et al.* (*5*) synthesized a series of binary metal oxides containing titanium by the coprecipitation method. The resultant oxides were found to show higher acid strength than each component oxide. Tanabe *et al.* (*6*) proposed a hypothesis to explain the formation of those acid sites; however, the materials themselves were not well characterized due to the amorphous nature of the solids. Since substitution with cations of lower oxidation states is expected to generate Brønsted acid sites, a series of titanium oxides doped with Cr(III) have been prepared in this experiment. For the purpose of correlating catalytic behavior to structure, the bimetallic oxides were synthesized by the coprecipitation method followed by hydro-

[1] To whom correspondence should be addressed.

0021-9517/90 $3.00
Copyright © 1990 by Academic Press, Inc.
All rights of reproduction in any form reserved.

thermal treatment to obtain crystalline materials. The technique used has been widely applied to prepare ZSM-like molecular sieves (*7*). A structure of high thermal stability was expected to be prepared by this technique. The acid/base properties of the resultant materials were characterized by infrared spectroscopy, temperature-programmed desorption (TPD) of ammonia, and 2-propanol decomposition reaction. Redox activity was examined by carrying out the oxidative dehydrogenation reaction of ethane.

METHODS

Reagents. Reagent-grade chemicals were used without further purification. $TiCl_4$ was purchased from Merck. $Cr(NO_3) \cdot 9H_2O$ was from Riedel-dehan. NH_3 gas for the TPD experiment was dried by passing it through a three-stage cold trap at 263 K and a NaOH column at room temperature.

Catalyst. A 5 *M* $TiOCl_2$ solution was prepared by dissolving $TiCl_4$ in 1 *N* HCl solution. It was used as the source of Ti(IV) in the following experiment. A powder of $Cr(NO_3)_3 \cdot 9H_2O$ was dissolved in 5 *N* NaOH solution. $TiOCl_2$ solution was then added dropwise into the solution with vigorous stirring. The final pH of the solution was adjusted to be higher than 12. The amorphous precipitate obtained was stirred for another 3 h, followed by hydrothermal treatment in a sealed polypropylene bottle at 373 K for 7 days. The green solid was filtered and washed with deionized water until it was free of Cl^- ions. The Brønsted acidic sites were formed by exchanging the incorporated Na^+ ions with an excess amount of NH_4^+ ions in 1 *M* NH_4Cl solution. The latter process was repeated three times at room temperature to achieve complete ion exchange, followed by washing and calcination at 623 K. The Cr(III) content was varied from 1, 5, 9, 15, 20, to 33% based on the starting Cr/(Ti + Cr) mole ratios. Component oxides of Ti(IV) and Cr(III) were also prepared separately for comparison in similar procedures.

Apparatus. X-ray powder diffraction patterns were obtained using a Philips 1792 X-ray diffractometer with Cu$K\alpha$ radiation. Infrared spectra were obtained with a Perkin–Elmer 983 spectrometer and a Bomen DA 3.02 FT-IR spectrometer. The wafers used for examining the stretching modes of surface hydroxyl groups and chemisorbed pyridine were 0.01 g/cm^2 thick. Measurement of surface area of the catalysts was based on the physical adsorption of nitrogen at liquid N_2 temperature using a volumetric system.

Procedures for TPD of NH_3. A 0.2-g portion of the catalyst was packed in a U-shape stainless-steel reactor. A thermocouple well was fixed at the center of the catalyst bed to register the temperature in the reaction zone. The catalyst was preheated under a dried N_2 atmosphere at 623 K for 1 h. NH_3 adsorption was carried out by passing dried NH_3 gas through the catalyst bed for 10 min at room temperature, followed by purging with N_2 gas for 30 min to drive excess NH_3 out the system. The TPD profile was obtained by heating the catalyst bed to 873 K at a heating rate of 10°K/min, and the amount of NH_3 desorbed was determined with a TCD detector.

Catalytic activity. The acid/base behavior of the catalysts was examined by carrying out the 2-propanol decomposition reaction in an ordinary plug-flow-type reactor at atmospheric pressure. Prior to the reaction, the calcined catalyst was reduced in a hydrogen stream at 623 K for 12 h to ensure that the catalyst had the chromium in the Cr(III) state. The rest of the procedures were same as those mentioned in a previous article (*8*). Redox activities of the catalysts were examined with the ethane oxidative dehydrogenation reaction in a plug-flow-type reactor at atmospheric pressure. The catalyst was preoxidized with air at reaction temperature, 723 K, for 12 h. A mixture of air/ethane in the ratio of 2/1 was used as reactant. The products were separated with a Porapak S column.

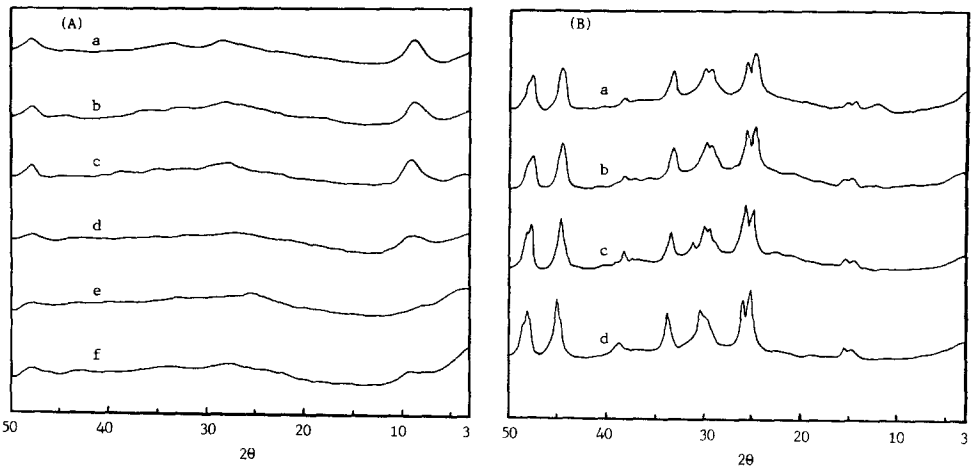

FIG. 1. XRD patterns of Cr–Ti oxides before (A) and after (B) calcination at 823 K. Cr/(Ti + Cr) ratios varied as (a) 0%, (b) 1%, (c) 5%, (d) 9%, (e) 15%, and (f) 20%.

RESULTS AND DISCUSSION

X-ray powder diffraction patterns showed that the synthesized bimetallic oxides had rather low crystallinities (Fig. 1A). Broadening peaks were observed at 2θ = 25, 37, and 48°, in addition to a peak at 2θ = 9° (d spacing = 9.8 Å). The latter became more obvious as the Cr(III) content was decreased. After calcination at 823 K for 4 h, the XRD patterns showed that crystalline phases were formed (Fig. 1B). The pattern could be assigned to Na_xTiO_2 bronze (*9*), except for peaks at 2θ = 25.2, 37, 37.8, and 48°, which were assigned to the anatase form of the TiO_2 phase.

Figure 2A shows the XRD patterns of samples after NH_4^+/Na^+ ion exchange. The crystallinity was found to remain low. However, the peak originally observed at low diffraction angle had shifted from 2θ = 9° to 2θ = 10°. Accordingly, the d spacing was found to shorten from 9.8 to 9.0 Å. After calcination at 623 K, anatase was the

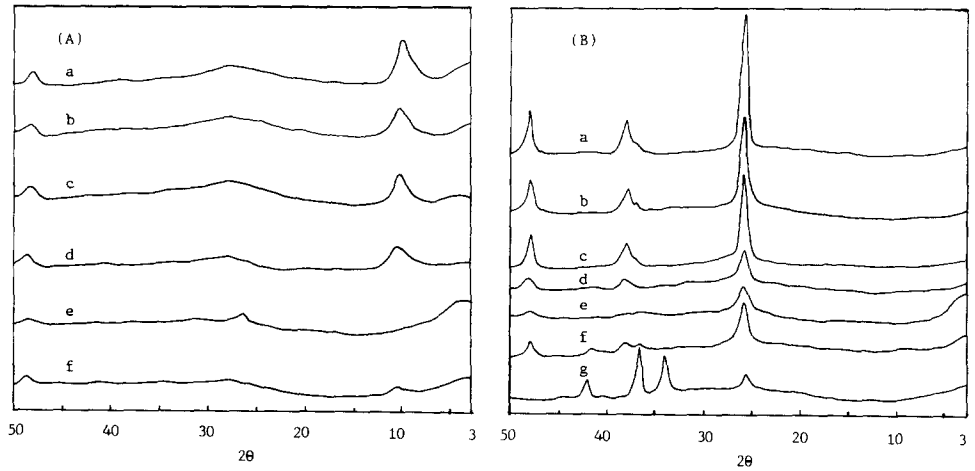

FIG. 2. XRD patterns of Cr–Ti oxides after NH_4^+/Na^+ ion exchange before (A) and after (B) calcination at 623 K. Cr/(Ti + Cr) ratios varied as (a) 0%, (b) 1%, (c) 5%, (d) 9%, (e) 15%, (f) 20%, and (g) 100%.

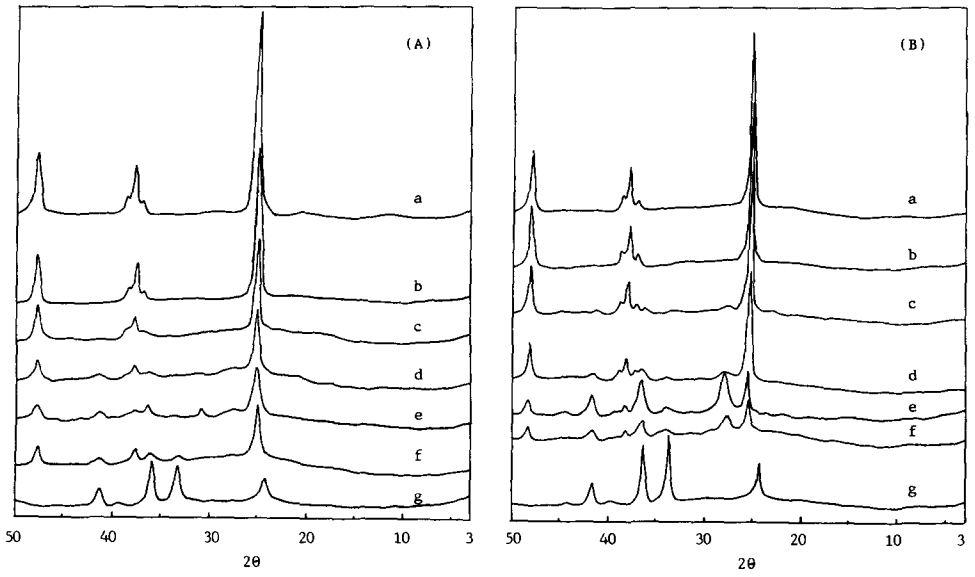

FIG. 3. XRD patterns of Cr–Ti oxides after NH_4^+/Na^+ ion exchange calcinated at (A) 723 K and (B) 943 K. Cr/(Ti + Cr) ratios varied as (a) 0%, (b) 1%, (c) 5%, (d) 9%, (e) 15%, (f) 20%, and (g) 100%.

only crystalline phase observed for samples with a Cr(III) content lower than 15%. As Cr(III) content was increased, a Cr_2O_3 phase was observed in addition to the anatase phase. Furthermore, the crystallinity obviously decreased as the Cr(III) content was increased. Calcining the samples at temperatures higher than 723 K induced formation of the rutile form of TiO_2 (Fig. 3). The latter was more obvious on samples with high Cr(III) content.

Figure 4 shows the infrared spectra of samples before and after NH_4^+/Na^+ ion exchange. NH_4^+ incorporation was indicated

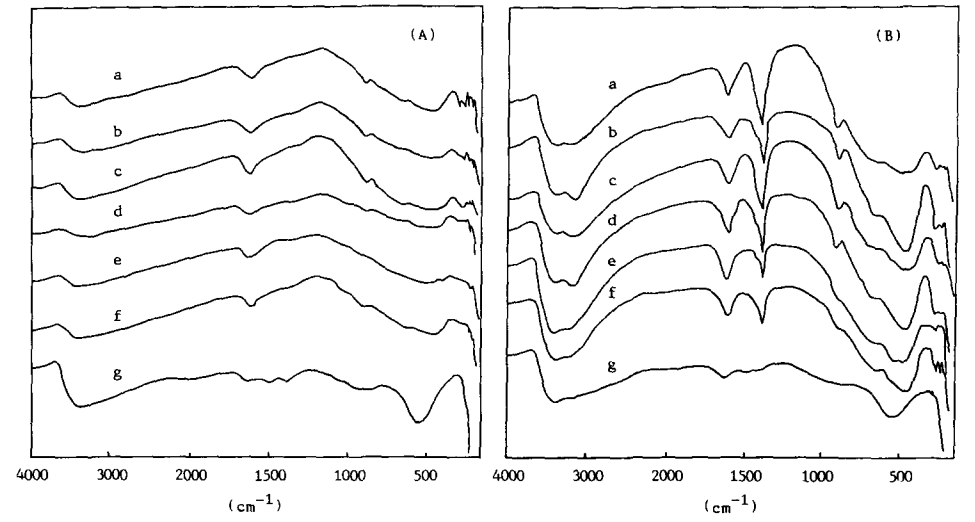

FIG. 4. IR spectra of Cr–Ti oxides before (A) and after (B) NH_4^+/Na^+ ion exchange. Cr/(Ti + Cr) ratios varied as (a) 0%, (b) 1%, (c) 5%, (d) 9%, (e) 15%, (f) 20%, and (g) 100%.

by the additional peaks that appeared at ca. 1400 and 3300 cm^{-1} on the exchanged samples. These peaks, which corresponded to the bending and stretching modes of N–H bonds, respectively, disappeared when the samples were calcined at 623 K.

The shift of the X-ray diffraction peak at low angle with the NH_4^+/Na^+ ion-exchange process indicated that the synthetic bimetallic oxides were layered structures. A series of layered titanates have been reported as inorganic ion exchangers (*10*). Izawa *et al.* (*11*) claimed that layered trititanate of the formula $Na_xH_{2-x}Ti_3O_7$ does not contain interlayer water and had interlayer distances that varied in the range 8.08–8.54 Å. Since those are smaller than what we have obtained, the structure of trititanate is ruled out. The other possible layered structure is tetratitanate. Sasaki *et al.* (*12*) studied the Na^+/H^+ ion-exchange process on hydrous tetratitanate. Compounds with the formula $Na_xH_{2-x}Ti_4O_9 \cdot 3.3H_2O$ had an interlayer distance of 11.2 Å. The partially dehydrated form, $NaHTi_4O_9 \cdot H_2O$, had an interlayer distance of 8.4 Å. The latter decomposed into a mixture of phases of sodium hexatitanate ($Na_2Ti_6O_{13}$) and anatase after heat treatment at 873 K. Since our samples have a *d* spacing of 9.8 Å, it is suspected that interlayer water molecules are more than 1 but less than 3 per formula. Furthermore, because layered titanates contain oxygen atoms of low coordination numbers (*10*), infrared spectra shall show Ti–O stretching at higher frequencies than that from anatase or rutile. Indeed, Fig. 4 shows that the IR spectra of the synthesized oxides have a rather sharp peak at 906 cm^{-1} near the Ti–O stretching band, which becomes negligible after the layered structure is collapsed through calcination.

The NH_4^+ tetratitanate is believed to release NH_3 on heating and transform to $H_2Ti_4O_9$ at rather low temperatures. The thermal decomposition of the latter compound has been well characterized by Izawa *et al.* (*11*). The reaction was proposed to be a dehydration reaction followed by phase transfer in the sequence of

$$H_2Ti_4O_9 \xrightarrow[-H_2O]{523\ K} H_2Ti_8O_{17} \xrightarrow[-H_2O]{<773\ K} TiO_2(B) \xrightarrow{773\text{–}1073\ K} TiO_2\ (\text{anatase})$$

where $TiO_2(B)$ has the same host lattice as that of Na_xTiO_2 bronze. Since the anatase phase was observed after the synthetic bimetallic oxides were calcined at 623 K, the phase transition processes on our samples seemed to occur at temperatures lower than that reported by Izawa *et al.* Furthermore, Cr(III) was considered to be incorporated into the lattice of anatase structure, especially when the Cr/Ti ratios were low. The lattice, however, was destabilized by Cr(III) substitution for Ti(IV) because the crystallinity decreased with the increase in Cr(III) content and a separate Cr_2O_3 phase was formed for samples of high Cr(III) content.

The BET surface areas of the synthesized oxides are tabulated in Table 1. Calcination caused the surface areas to shrink from ca. 200 m^2/g to ca. 110 m^2/g at 623 K, and to less than 75 m^2/g at 723 K. On the other hand, the surface areas are larger for samples of higher Cr(III) content. These phenomena can be correlated with the variation in crystallinity.

TABLE 1

BET Surface Areas of the Catalysts after NH_4^+/Na^+ Ion Exchange

Cr/(Ti + Cr) (%)	BET surface area (m^2/g)			
	Before calcination	Calcination		
		623 K	723 K	943 K
0	256	95	65	58
1	185	106	—	32
5	187	118	43	50
9	195	117	71	65
20	218	166	75	70
100	—	54	42	—

TABLE 2

Kinetic Data of 2-Propanol Decomposition over Cr–Ti Oxides[a]

Cr/(Ti + Cr) (%)	R_p/R_a (cm³/g · min)				E_{a_p} (kcal/mol)	E_{a_a} (kcal/mol)
	493 K	523 K	553 K	583 K		
	(cm³/g · min)					
0	0.42/—	1.83/ 0.15	13.3 / 0.74	48.0/ 1.97	30.4	26.5
1	—	0.25/ 0.21	1.76/ 1.26	13.4/ 5.70	40.2	33.4
5	0.26/0.56	0.78/ 1.55	5.67/ 7.89	33.0/27.3	31.4	25.2
9	0.35/1.06	1.36/ 3.40	16.7 /12.4	88.6/48.7	36.2	24.2
20	0.26/1.64	1.71/ 5.42	9.72/14.2	65.3/42.8	34.9	20.6
100	3.07/7.72	15.4 /21.2	31.8 /29.4	89.3/70.4	21.2	13.5

[a] R_p = rate of propylene formation; R_a = rate of acetone formation; E_{a_p} = activation energy of propylene formation; E_{a_a} = activation energy of acetone formation.

Both propylene and acetone were obtained as products when 2-propanol was decomposed over the synthesized oxides. This implies that the oxides contain both acidic and basic sites. The kinetic data were analyzed according to first-order kinetics in a plug-flow reactor. Table 2 lists the calculated rate constants for the formation of propylene and acetone, respectively, over the samples of various Cr(III) content after calcination at 623 K. Among them, pure chromium oxide demonstrated the highest activities in both dehydrogenation and dehydration reactions. On the other hand, pure titanium oxide shows fair activity in dehydration reaction, but the lowest activity in dehydrogenation reaction. Moreover, the selectivity to propylene was found to be affected by the Cr(III) content, as illustrated in Fig. 5. The products contained more than 92% ethylene over pure titanium oxide. The value dropped sharply when a very small quantity of Cr(III) was doped into the catalyst. Therefore, it is proposed that the basic sites are associated with Cr(III) ions, which substitute for Ti(IV) ions in the anatase lattice.

The surface acid strength of the mixed oxides was determined by temperature-programmed desorption of ammonium (Fig. 6). The NH_3 molecules desorbed at temperatures lower than 473 K are considered due to physical adsorption on the surface. Pure titanium oxide shows another desorption maximum at 558 K. Pure chromium oxide has a maximum at 638 K. While the sample with 1% Cr(III) has only one maximum at 493 K, the rest of the Cr/Ti bimetallic oxides show two maxima: one at ca. 493–513 K and the other at ca. 573–583 K. Accordingly, pure chromium oxide has the strongest acidic sites and the sample with 1% Cr(III) has the weakest acidic sites. The activation energies calculated for 2-propanol dehydration reaction (Table 2) were found to vary in a similar trend.

Infrared spectra in the O–H stretching region of the calcined samples are illus-

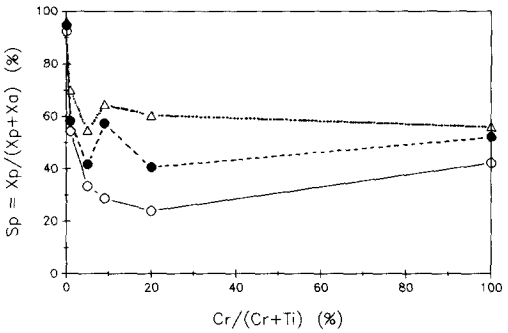

FIG. 5. Selectivities of propylene over total conversion in 2-propanol decomposition reaction over Cr–Ti oxides as a function of Cr/(Ti + Cr) ratio. ○, 523 K; ●, 553 K; △, 583 K.

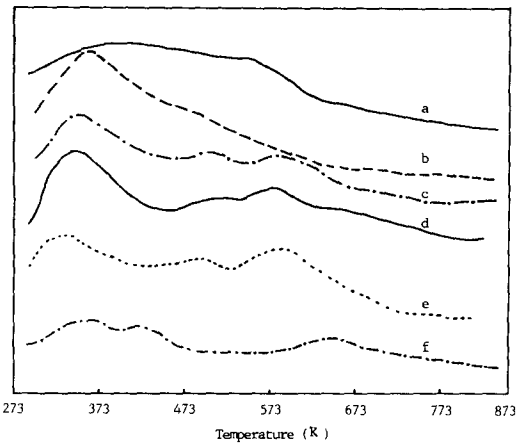

FIG. 6. Temperature-programmed desorption profiles of NH_3 over Cr–Ti oxides. Cr/(Ti + Cr) ratios varied as (a) 0%, (b) 1%, (c) 5%, (d) 9%, (e) 20%, and (f) 100%.

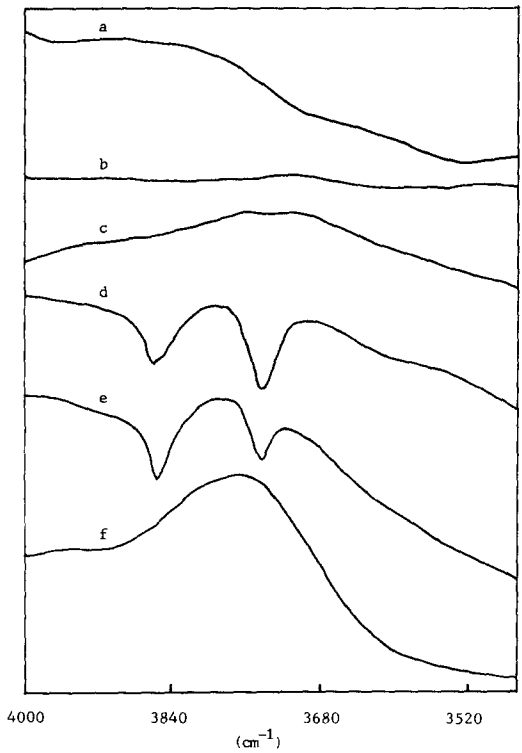

FIG. 7. FT-IR spectra of Cr–Ti oxide wafers after evacuation at 623 K for 1 h. Cr/(Ti + Cr) ratios varied as (a) 0%, (b) 1%, (c) 5%, (d) 9%, (e) 20%, and (f) 100%.

trated in Fig. 7. Two peaks were observed at 3749 and 3855 cm^{-1}, respectively, on the samples of Cr(III) content 9 and 20%. The rest of the samples showed negligible absorption in this region. Judging from the charge density of the lattice cations, the peak at 3749 cm^{-1} is assigned to TiO–H stretching and 3855 cm^{-1} to CrO–H stretching. Parkyns summarized the IR frequencies of surface hydroxyl groups on titania reported by several authors (*13*). TiO–H stretching frequencies ranged from 3668 to 3740 cm^{-1} depending on the heat treatment and the crystalline phases. The values are close to the 3749 cm^{-1} observed on our samples. On heating to 723 K and 943 K, the peak at 3855 cm^{-1} became weaker while that at 3749 cm^{-1} was retained (Fig. 8). To study the nature of the acid sites, infrared spectra of pyridine adsorbed on the surface of the mixed oxides were examined. Figure 9A is the spectra of the sample with 9% Cr(III) after calcination at 623 K. There were peaks at 1440, 1443, 1477, 1492, 1553, 1578, 1596, and 1604 cm^{-1} comprising the vibrational modes of pyridine. Among them, peaks at 1443, 1492, 1578, and 1596

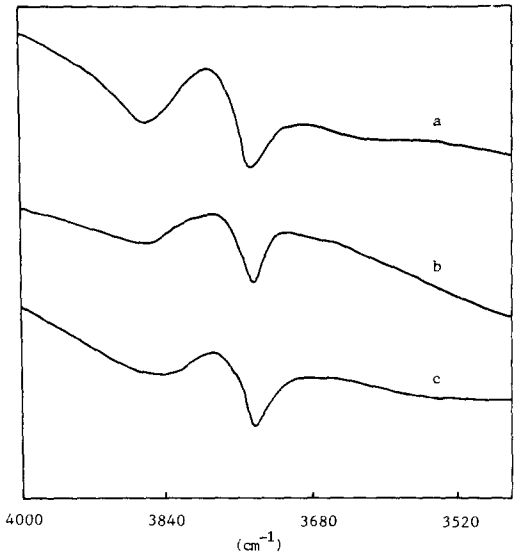

FIG. 8. FT-IR spectra of Cr–Ti oxides with Cr/(Ti + Cr) ratio of 9% after evacuation at (a) 623 K, (b) 723 K, and (c) 943 K.

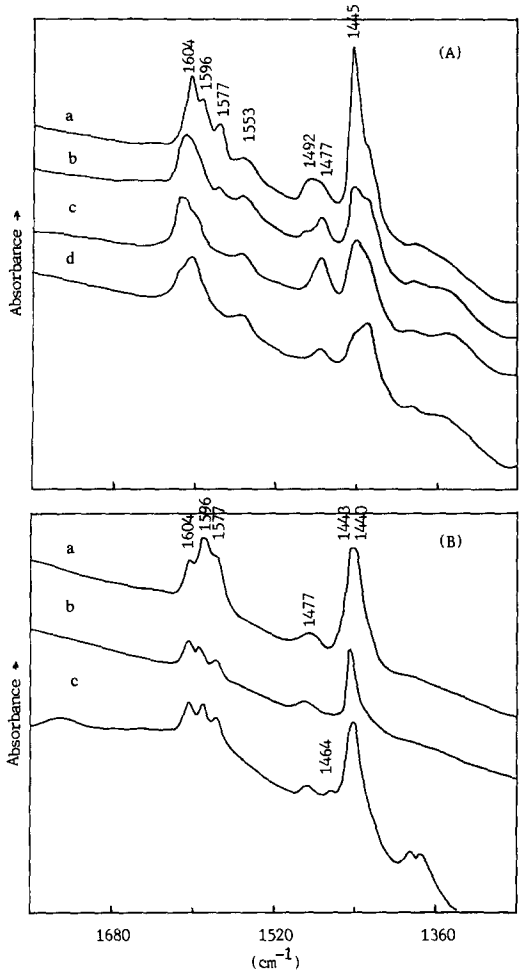

FIG. 9. FT-IR spectra of pyridine adsorbed on calcined Cr–Ti oxide (Cr/(Ti + Cr) = 9%) after evacuation at (a) RT (b) 423 K, (c) 523 K, and (d) 623 K. The calcination temperatures were (A) 623 K and (B) 723 K.

cm^{-1} were weakened after evacuation at 423 K, and almost disappeared after evacuation at 523 K. According to Kung and Kung (*14*), this set of absorption peaks can be assigned to hydrogen-bonded pyridine. On the other hand, a new peak appeared at 1613 cm^{-1} on heating. That and the rest of peaks survived even at an evacuation temperature of 623 K. Connell and Dumesic (*15*) indicated that peaks at 1553 and 1613 cm^{-1} were the characteristic peaks of pyridinium ions, which were formed on the Brønsted acid sites. The other set of absorption peaks at 1440, 1477, and 1604 cm^{-1} was contributed by pyridine coordinatively bonded to Lewis acid sites. Figure 9B shows the IR spectra of pyridine adsorbed on the same sample calcined at 723 K. Peaks attributed to hydrogen-bonded pyridine at 1443, 1492, 1577, and 1596 cm^{-1} were observed in addition to those from Lewis acid sites at 1440, 1477, and 1604 cm^{-1}. We conclude that both Brønsted and the Lewis acid sites exist on the surface of the bimetallic oxides after calcination at 623 K, but the bimetallic oxides lose the Brønsted acid sites after calcination at 723 K. TiO–H groups are still observed on the latter compounds, which implies that the TiO–H groups do not contribute to the Brønsted acidity. In other words, the Brønsted acid sites are the CrO–H groups.

Figure 10 demonstrates the redox activi-

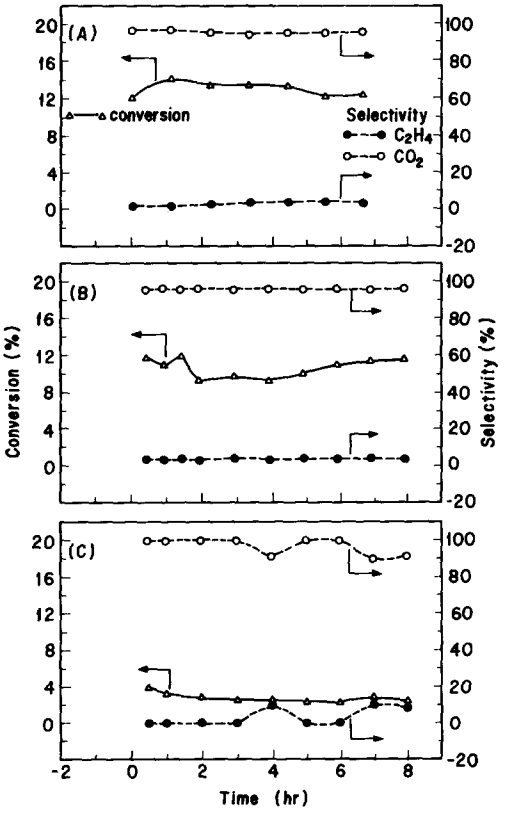

FIG. 10. Activities of Cr–Ti oxides in ethane oxidative dehydrogenation reaction. Catalysts had Cr/(Ti + Cr) ratios of (a) 100%, (b) 20%, and (c) 5%.

ties of the bimetallic oxides in the oxidative dehydrogenation of ethane. Besides the desired product, ethylene, carbon dioxide was obtained as a major product through complete oxidation of ethane or ethylene. The conversion was found to be proportional to the Cr content of the oxides. Pure chromium oxide gave the highest activity. The total conversion of ethane was ca. 14 mol%. However, only 4 mol% of the products was ethylene. On the other hand, the selectivity of ethylene was found to be independent of Cr content. It is therefore proposed that the active sites for the formation of ethylene and CO_2 are the same and may have to do with surface Cr–O species. Ti(IV) served more as a diluent.

CONCLUSIONS

Cr(III)/Ti(IV) bimetallic oxides prepared by the hydrothermal method in basic solution were found to have layered structures. After NH_4^+/Na^+ ion exchange and calcination, the tetratitanate was converted to anatase-form TiO_2 structure. Cr(III) ions were proposed to substitute for the Ti(IV) ions in the lattice. As a result, the crystallinity of the anatase phase decreased with the increase in Cr(III) content. A separate Cr_2O_3 phase was also observed on samples of high Cr(III) content. Over pure titanium oxide, propylene was the predominant product obtained in the 2-propanol decomposition reaction. Selectivity decreased sharply when a very small quantity of Cr(III) was doped into the oxide. Since both propylene and acetone were obtained in the products, it was concluded that the synthetic bimetallic oxides contain both acidic and basic sites. Furthermore, there were two kinds of acid sites on the bimetallic oxides—Brønsted and Lewis. The Brønsted acid sites were determined to be the CrO–H groups on the surface. The Cr–O species were also proposed to be the active sites for the oxidative dehydrogenation of ethane to ethylene and for complete oxidation to CO_2.

ACKNOWLEDGMENT

Financial support from the National Science Council of the Republic of China is gratefully acknowledged.

REFERENCES

1. Tauster, S. J., Fung, S. C., and Garden, R. L., *J. Amer. Chem. Soc.* **100,** 170 (1978).
2. Matsuda, S., Takeuchi, M., Hishinuma, T., Nakajima, F., Narita, T., Watanabe, Y., and Imanati, M., *J. Air Pollut. Control Assoc.* **28,** 350 (1978).
3. Inomata, M., Miyamoto, A., and Murakami, Y., *J. Chem. Soc. Chem. Commun.*, 223 (1980).
4. Matsuda, S., and Kato, A., *Appl. Catal.* **8,** 149 (1983).
5. Shibata, K., Kitagawa, T., Sumiyoshi, T., and Tanabe, K., *Bull. Chem. Soc. Japan* **46,** 2985 (1973).
6. Tanabe, K., Sumiyoshi, T., Shibata, K., Kiyoura, T., and Kitagawa, J., *Bull. Chem. Soc. Japan* **47,** 106 (1974).
7. Gbelica, Z., Derouane, E. G., and Blom, N., *in* "Catalytic Materials," Chap. 12. Amer. Chem. Soc., Washington, DC, 1984.
8. Cheng, S., and Lee, J.-C., *J. Chin. Chem. Soc.* **35,** 191 (1988).
9. Marchand, R., and Brohan, L., *Mater. Res. Bull.* **15,** 1129 (1980).
10. Izawa, H., Kikkawa, S., and Koizumi, M., *Polyhedron* **2,** 741 (1983).
11. Izawa, H., Kikkawa, S., and Koizumi, M., *J. Phys. Chem.* **86,** 5023 (1982).
12. Sasaki, T., Watanabe, M., and Fujiki, Y., *Bull. Chem. Soc. Japan* **58,** 3500 (1985).
13. Parkyns, N. A., *in* "Chemisorption and Catalysis" (P. Hepple, Ed.). Elsevier, Amsterdam, 1970.
14. Kung, M. C., and Kung, H. H., *Catal. Rev.-Sci. Eng.* **3,** 425 (1985).
15. Connell, G., and Dumesic, J. A., *J. Catal.* **105,** 285 (1987).